



OPEN

SUBJECT AREAS:

NANOWIRES

CARBON NANOTUBES AND
FULLERENESReceived
27 February 2014Accepted
9 April 2014Published
25 April 2014

Correspondence and
requests for materials
should be addressed to
J.T.H. (jthan@keri.re.
kr) or G.-W.L.
(gwleephd@keri.re.kr)

Electrically Robust Metal Nanowire Network Formation by In-Situ Interconnection with Single-Walled Carbon Nanotubes

Jong Seok Woo¹, Joong Tark Han^{2,3}, Sunshin Jung¹, Jeong In Jang¹, Ho Young Kim¹, Hee Jin Jeong¹, Seung Yol Jeong¹, Kang-Jun Baeg¹ & Geon-Woong Lee¹

¹Nano Hybrid Technology Research Center, Korea Electrotechnology Research Institute (KERI), Changwon 642-120, Republic of Korea, ²Multidimensional Nanomaterials Research Group, Korea Electrotechnology Research Institute (KERI), Changwon 642-120, Republic of Korea, ³Department of Electrical Functionality Material Engineering, University of Science and Technology (UST), Daejeon, 305-333, Republic of Korea.

Modulation of the junction resistance between metallic nanowires is a crucial factor for high performance of the network-structured conducting film. Here, we show that under current flow, silver nanowire (AgNW) network films can be stabilised by minimizing the Joule heating at the NW-NW junction assisted by in-situ interconnection with a small amount (less than 3 wt%) of single-walled carbon nanotubes (SWCNTs). This was achieved by direct deposition of AgNW suspension containing SWCNTs functionalised with quadruple hydrogen bonding moieties excluding dispersant molecules. The electrical stabilisation mechanism of AgNW networks involves the modulation of the electrical transportation pathway by the SWCNTs through the SWCNT-AgNW junctions, which results in a relatively lower junction resistance than the NW-NW junction in the network film. In addition, we propose that good contact and Fermi level matching between AgNWs and modified SWCNTs lead to the modulation of the current pathway. The SWCNT-induced stabilisation of the AgNW networks was also demonstrated by irradiating the film with microwaves. The development of the high-throughput fabrication technology provides a robust and scalable strategy for realizing high-performance flexible transparent conductor films.

One-dimensional (1D) nanomaterials, such as silver nanowires (AgNWs) or carbon nanotubes (CNTs), have been investigated as alternative electrode materials for fabricating transparent conducting films (TCFs) on plastic substrates instead of the brittle and expensive indium tin oxide¹⁻⁸. The electrical conduction of these network films composed of 1D materials is typically dominated by the tube-tube or NW-NW junction resistance^{7,9,10}. Under high current flow, the relatively high junction resistance between the metal NWs exerts a detrimental effect on the network stability, resulting in the breaking up of the NWs at the junction^{11,12}. Self-joining of the network junctions can be one solution to solve the issues encountered with stability and to enhance the electrical conductivity of the film via post treatment^{9,10,13}. Another strategy is to interconnect the NWs with other conducting materials or metal oxides¹⁴⁻²⁶. However, these processes require additional steps, such as irradiation with light, heating at high temperatures and the removal of surfactant molecules after the deposition of AgNWs or AgNW hybrid materials.

We suggest that a small amount of less defective single-walled CNTs (SWCNTs) with small bundle structures, because of their high thermal conductivity and stability, can be used as a good networking material to enhance the stability of AgNW networks under current flow. The major challenge in producing a well-distributed AgNW/SWCNT hybrid film by a high-throughput process is the fabrication of a stable dispersion of SWCNTs in the medium of the AgNW dispersion. Without dispersion agents, hydrophobic SWCNTs aggregate in aqueous or alcoholic media used to disperse AgNWs. If insulating surfactant molecules are used for dispersion, an additional step involving their removal is required to prepare high performance TCFs. Moreover, it is challenging to overcome the van der Waals interaction between the nanotubes in an aqueous solution without dispersant. However, severe functionalisation of nanotubes is disadvantageous because the overall properties (e.g., the



electrical and thermal properties) of the resulting films can suffer because of the decreased electrical conductivity of the SWCNTs.

Here we show that the solution mixture for thin film deposition can be prepared by the direct mixing of less defective SWCNTs functionalised with quadruple hydrogen bonding (QHB) motifs with an aqueous suspension of AgNWs. This enabled the preparation of well-distributed AgNW/SWCNT hybrid films by direct deposition of the solutions on plastic substrates without further treatments. Importantly, we demonstrate that under current flow, the AgNW network films were stabilised by interconnection with SWCNTs without the requirement of additional treatments via the modulation of the electrical current pathway. The stabilisation mechanism of the AgNW/SWCNT hybrid films was explored by fabricating thin film heaters and by irradiating the films with microwaves (MWs) to trigger an immediate Joule heating of AgNWs and SWCNTs on the film.

Results

High-throughput fabrication of the AgNW/SWCNT hybrid film.

Figure 1a is the schematic representing the preparation of the solution containing the AgNW and SWCNT mixture. First, SWCNTs were dispersed in dimethylformamide in the form of a paste (10 wt% solid content), without the addition of any other dispersant molecules. This was realised by attaching QHB motifs of 2-ureido-4[1H]pyrimidinone (UHP) moieties through a previously reported sequential coupling reaction²⁷. During the initial acid treatment step, the defect formation in SWCNTs was minimized by a mild treatment at low temperatures (50°C). The SWCNTs functionalised with carboxylic acid groups were subjected to reaction with toluene diisocyanate and 2-amino-4-hydroxy-6-methyl-pyrimidine sequentially to attach the isocyanate and UHP groups, respectively (Supplementary Fig. S1). The paste of SWCNTs having QHB motifs (QHB-SWCNTs) was directly added into the aqueous AgNW suspension (0.5 wt%) (Supplementary Fig. S2) with shaking, as shown in Figure 1a. The resulting solution was stable without any other additional dispersion agent for dispersing SWCNTs. This may be

realized by the solvation of dissociated UHP-functionalised SWCNTs (UHP-SWCNTs) by water molecules. The solution was directly spray coated on polycarbonate substrates to fabricate the flexible TCFs, as shown in Figure 1b. The Raman spectrum in Figure 1c shows the co-existence of SWCNTs and AgNWs in the film. Importantly, the D/G ratio of the QHB-SWCNTs was as low as 0.01, which indicates that the QHB formation process occurred by minimizing the defect formation on the nanotube surface. The tilted top-view scanning electron microscope (SEM) images show that the AgNWs were homogeneously interconnected with the SWCNTs in the film (Figs. 2a to d). By increasing the AgNW/SWCNT densities on the polycarbonate substrates, the sheet resistance (R_s) \approx 13 Ω /sq and $T \approx$ 90.2% could be achieved (Fig. 2e), which is comparable to those of the previously reported TCFs that showed the best performance^{4,23}. This is consistent with the predicted contact resistance (2 k Ω) between AgNWs and their aspect ratio (\sim 700)⁴. Notably, after the addition of about 3 wt% of SWCNTs, R_s of the AgNW network film did not increase at the same transmittance, and irrespective of the transmittance, more current flowed through the hybrid film (Fig. 2f). However, when more SWCNTs were incorporated in the AgNW networks, the optical absorption increased and the contact between AgNWs decreased, which resulted in an increase in R_s of the film.

Electrical stabilisation of AgNW networks with carbon nanotubes.

To demonstrate the effect of the SWCNTs on the electrical stability of the AgNW films under current flow, we fabricated transparent film heaters on flexible plastic substrates. The films with R_s of \sim 20 Ω /sq and $T >$ 90% was used to fabricate the transparent film heaters. Figure 3 shows the heating behavior of the films as a function of time and the infrared images of the fabricated AgNW-based film heaters at applied input voltages are furnished. In the case of the AgNW network films (without the SWCNTs), even at a low input voltage (of 9 V), hot spots and temperature drop could be observed even at low temperatures (of \sim 75°C) (Fig. 3a). However, by

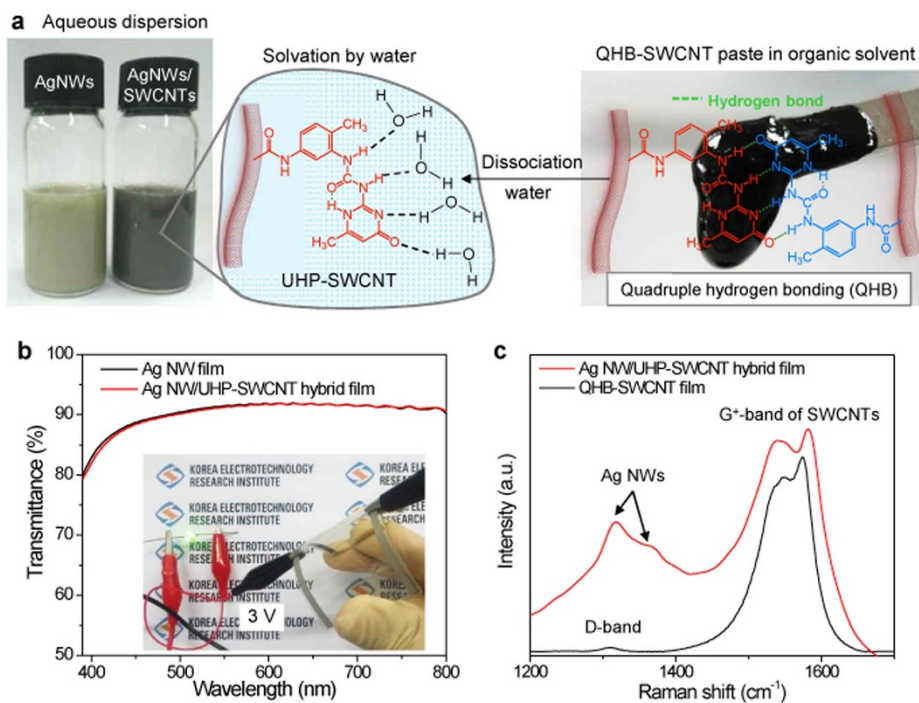


Figure 1 | Dispersant-free fabrication of AgNW/SWCNT hybrid films. (a) A schematic representing the fabrication procedures used for preparing a stable AgNW/SWCNT mixture. (b) Optical transmission of the AgNW and AgNW/SWCNT hybrid films with $R_s \approx$ 20 ohm/sq. The inset image shows the banded AgNW/SWCNT hybrid film on a polycarbonate substrate lighting the LED lamp at 3 V. (c) Raman spectra of the QHB-SWCNT and AgNW/UHP-SWCNT hybrid films.

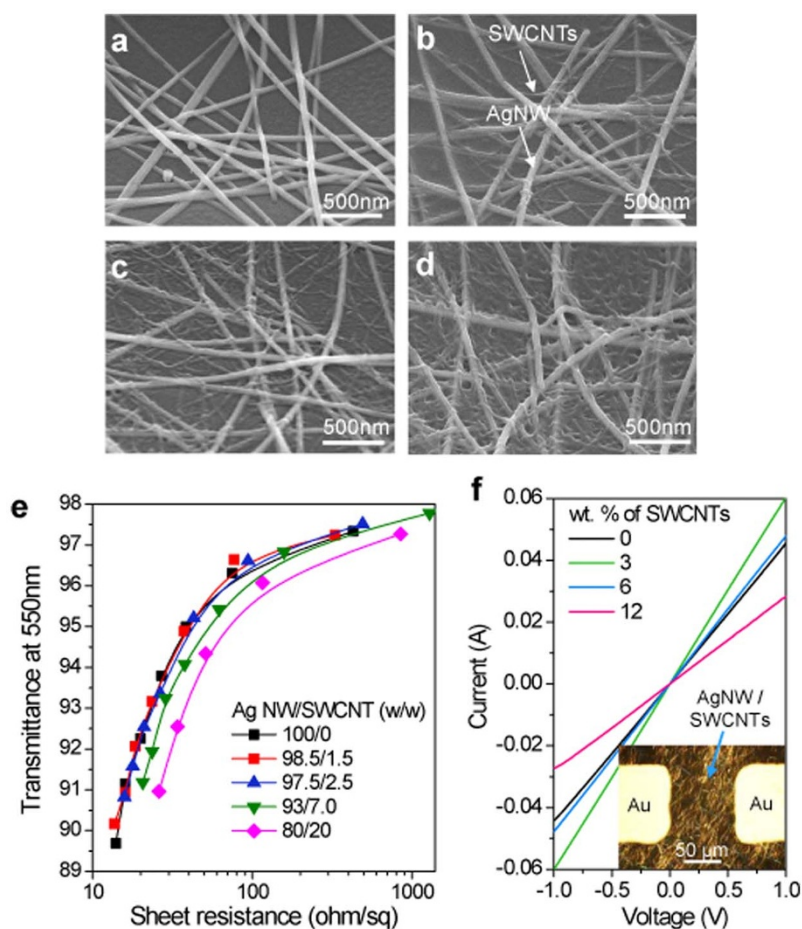


Figure 2 | Characterization of the film. Tilted SEM images of the (a) AgNW film and AgNW/SWCNT hybrid films incorporating different amounts of SWCNTs; (b) 2.5, (c) 7.0, and (d) 20 wt%. (e) Plot of T (550 nm) vs. R_s for AgNW and AgNW/SWCNT hybrid films containing various amounts of SWCNTs. (f) I-V plots of pristine AgNW and AgNW/SWCNT hybrid films.

incorporating 2.5 wt% of SWCNTs in the AgNW networks, stable heating was realized even at 15 V, as shown in Figure 3b. To understand the reason behind the generation of hot spots in the film, we characterized the hot spot region by SEM. Notably, we could observe the breaking up of AgNWs at junctions (Fig. 3c), which might have been induced by rapid Joule heating at the junctions because of the high junction resistance of the AgNWs^{11,12}. In stark contrast, the AgNWs in hybrid films were very stable even after applying 15 V (Fig. 3d and supplementary Fig. S3). However, although a smaller amount of SWCNTs (1.5 wt%) in the AgNW networks did work as a stabiliser at 9 V, hot spots were observed in the film from 11 V (Supplementary Fig. S3). In addition, the AgNW/SWCNT hybrid films were found to be mechanically stable from the taping tests (Supplementary Fig. S4) because of the thermal welding or embedding of the AgNWs and SWCNTs into the plastic substrate during the current-induced heating. Finally, by applying a low voltage to the film (5 V), we observed the decolouring of the thermochromic material pattern (red color), which reacted at low temperatures (40 °C) (Supplementary Fig. S5). When a higher voltage (of 7 V) was applied, the blue colored pattern decoloured at 60 °C. These decoloured patterns were recovered at 0 V.

As mentioned earlier, the unstable heating and hot spot formation in the AgNW films under current flow are related to the high contact resistance between the AgNWs. In the AgNW film, the high NW-NW contact resistance ($R_{11} \approx 10^3 \sim 10^9 \Omega$) and poor contact can induce high Joule heating at the junctions under the applied voltage, resulting in hot spot formation and breaking up of the AgNWs^{10,11}.

However, as illustrated in Figure 3e, by interconnecting the AgNWs with the SWCNTs, we can modulate the current pathway through the NW-SWCNT junction because of the relatively low contact resistance between the AgNW and SWCNT ($R_{12} \approx 10^3 \Omega$) when compared to R_{11} (Supplementary Fig. S6)²⁸. Moreover, highly flexible SWCNTs have more contact area than AgNWs do, as illustrated in Figure 4a and b. Due to the high thermal conductivity of the SWCNTs, a higher amount of SWCNTs in the AgNW networks may also act as thermal spreaders and network stabilisers in the film heaters even at high voltages. Furthermore, we measured the work function (Φ) values of AgNWs and UHP-SWCNTs by using UV photoelectron spectroscopy (UPS). The Φ values were estimated from the secondary electron cutoff using the relation $\Phi = h\nu - (E_F - E_{\text{cutoff}})$, where $h\nu$, E_F , and E_{cutoff} are the photon energy of the excitation light (21.22 eV), the Fermi level edge, and the measured secondary electron cutoff, respectively. Very small work function difference practically exists in the contact between AgNW and UHP-SWCNTs based on the Φ values of AgNW (4.1 eV) and UHP-SWCNTs (4.3 eV) (Fig. 4c). The secondary amine groups in UHP moieties may decrease the Φ value of UHP-SWCNTs, which was increased to 4.5 eV after thermal treatment at 250 °C under vacuum. Thus, we propose that good contact and Fermi level matching between AgNWs and UHP-SWCNTs lead to the modulation of the current pathway (Fig. 4d).

Electrical stability under microwave irradiation. To further demonstrate the stabilisation mechanism, the AgNW and AgNW/

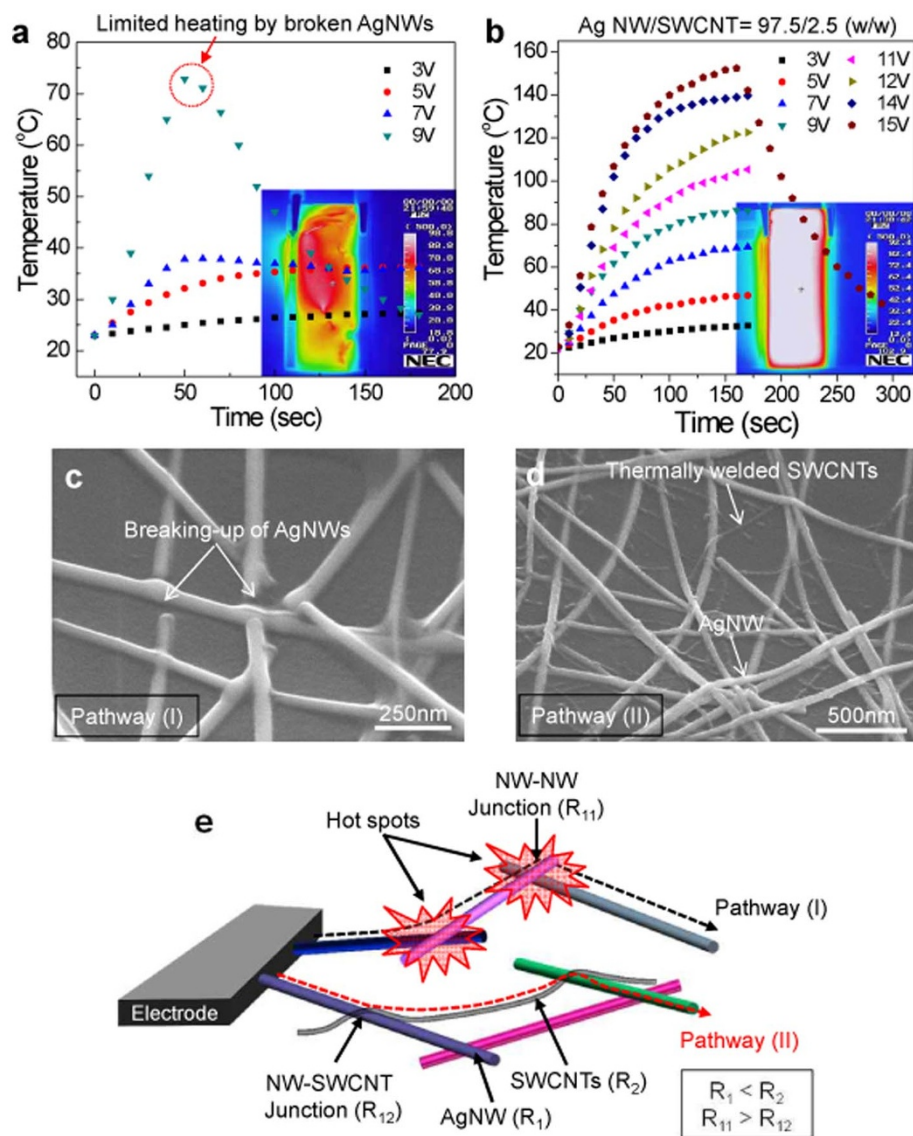


Figure 3 | Film stability under the current flow. Time dependent temperature profiles of (a) AgNW and (b) AgNW/SWCNT hybrid films. The inset images are the infrared thermal images of the film heaters. Tilted SEM images of (c) AgNW and (d) AgNW/SWCNT hybrid films after heating at an input voltage of 9 V. (e) Schematic of the AgNW/SWCNT hybrid networks showing the possible current flow pathway (I, II). R_1 and R_2 indicate the resistivity of AgNWs and SWCNTs, respectively. R_{11} or R_{12} indicate the contact resistances between AgNWs or between an AgNW and SWCNTs.

SWCNT hybrid films were irradiated with MWs inside the rectangular waveguide MW applicator, where the MW electric field was well-defined and controlled (Supplementary Fig. S7)²⁹. The electric field of the MW could efficiently induce a rapidly oscillating current in the film and the AgNWs and SWCNTs directly interacted with the MWs, resulting in an immediate flash Ohmic heating by the induced current. Moreover, the induced current can flow at the junctions of the AgNWs or SWCNTs in the film. Thus, a small NW-NW or NW-SWCNT junction resistance can ensure stable heating by MW irradiation. Figure 5a shows the temperature change of the AgNW and AgNW/SWCNT hybrid films under MW irradiation as a function of time. Interestingly, in the AgNW film, we could observe a saw-like temperature profile, as indicated by arrows, while the AgNW/SWCNT hybrid film showed a stable and rapid increase of temperature under MW irradiation. Interestingly, the undesirable breaking up of AgNWs at the junctions was observed in the AgNW film (inset image in Fig. 5a). This result clearly shows that the high temperature heating at the NW-NW junction by Joule heating occurred because of the high contact resistance. However, as shown in Figure 5b, most of the

AgNWs in AgNW/SWCNT hybrid film were stable even after heating to 160 °C by MW irradiation. This indicates that the MW-induced current at the junction flowed through the AgNW and SWCNT junctions as illustrated in Figure 5c. Therefore, we believe that the interconnecting SWCNTs played the role of junction modifiers in the AgNW network film and stabilised the film under current flow.

Discussion

In summary, to stabilise AgNW films under heating by DC voltage, we modulated the AgNW network with SWCNTs, which was realized by direct deposition of the films from a stable AgNW/SWCNT dispersion in aqueous medium. This was achieved by directly mixing SWCNTs functionalised with QHB moieties with an aqueous AgNW suspension. The AgNWs were uniformly interconnected with the SWCNTs, which dramatically stabilised the AgNW networks even at high input voltages, resulting in high-temperature heating. The stabilisation mechanism involves the modulation of the electrical transportation pathway in the film by the SWCNTs interconnecting the AgNWs by good contact and Fermi level matching between

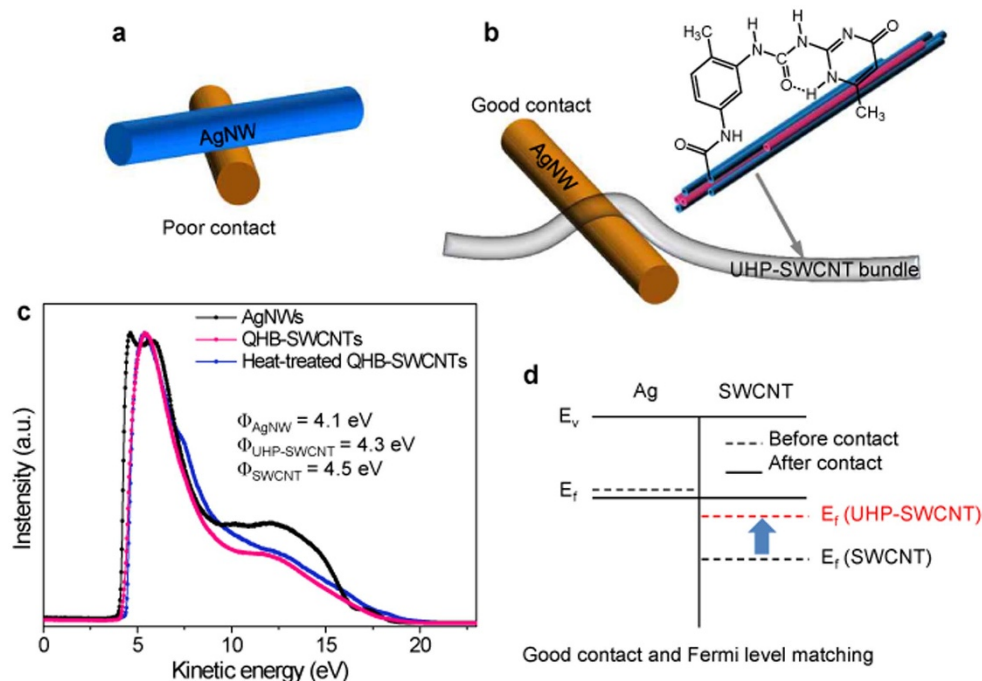


Figure 4 | Wettability and Fermi level matching. Schematics of contact forms with metals of (a) AgNWs and (b) AgNW/SWCNTs. (c) UPS spectra of the AgNW, UHP-SWCNT, and thermally-treated UHP-SWCNT films. (d) Schematics of the reduced contact barrier formation with metals of AgNW and UHP-SWCNTs.

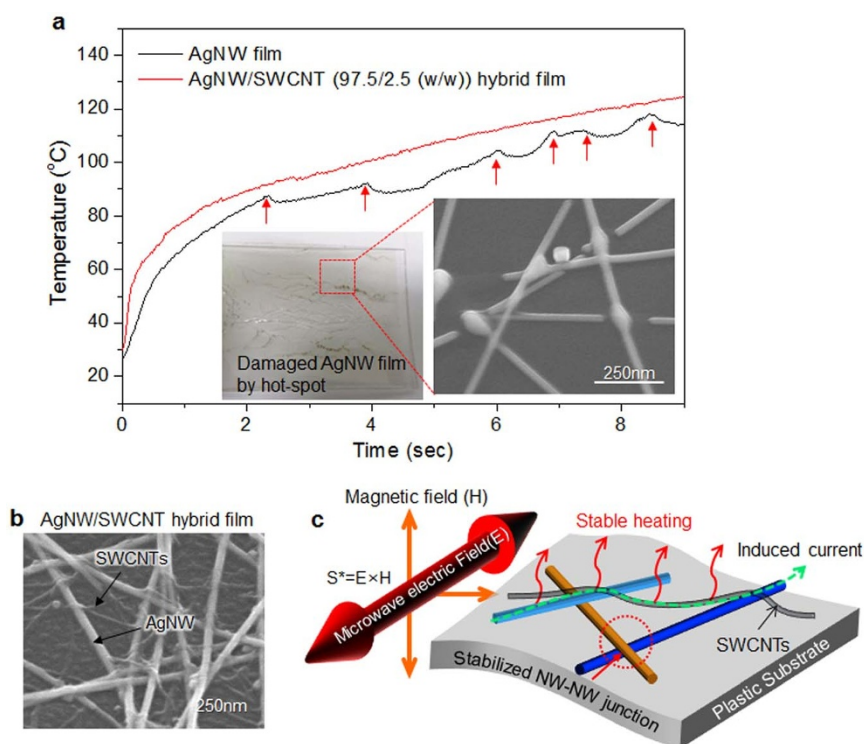


Figure 5 | AgNW network stability under microwave irradiation. (a) Temperature profile of the AgNW and AgNW/SWCNT hybrid films as a function of time under MW radiation at a power of 10 W. Inset images show the photograph (left) and the SEM image (right) of the AgNW film after MW irradiation. (b) Tilted SEM images of the stable AgNW/SWCNT hybrid films after MW irradiation. (c) Schematic illustration of stable heating of the AgNW/SWCNT hybrid film through the modulated current pathway created by SWCNTs interconnecting the AgNWs, wherein the microwave electric field is parallel to the film. The green arrow indicates the flow of the induced current through the AgNWs to the SWCNTs by MW irradiation.



AgNWs and modified-SWCNTs. The SWCNT-induced stabilisation of the AgNW networks was also demonstrated by irradiating the films with MWs. We believe that the high-throughput fabrication technology proposed here provides a robust and scalable strategy for realizing high-performance flexible transparent conducting electrode films.

Methods

Preparation of the AgNW and SWCNT solution and film fabrication. AgNWs with an average length of 25 μm and average diameter of 35 nm (Figure S2), dispersed in water (0.5 wt%) were purchased from Nanopixys Inc. and used as received. SWCNTs produced by the arc-discharge method and purified by thermal treatment (purchased from Nano Solution, Extube) were used as interconnecting materials of AgNW networks without further separation of semiconducting and metallic SWCNTs. The SWCNT paste stabilised by QHBs was prepared in three steps as previously reported (Figure S1). The SWCNTs functionalised with carboxylic acid groups which were dispersed (3 g/L) in dimethylformamide (DMF) was allowed to react with an excess amount (4 mL) of toluene diisocyanate (Aldrich) at 50 °C for 24 h under Ar purging to obtain the isocyanate-modified SWCNTs (SWCNTs-NCO). Subsequently, 500 mL of the SWCNTs-NCO dispersion in DMF was allowed to react with 2-amino-4-hydroxy-6-methyl-pyrimidine (Aldrich) (1.8 g) in the presence of 4 mL of triethylacetate (catalyst) at 100 °C for 20 h under magnetic stirring. The modified SWCNTs were then purified by centrifugation and vacuum filtration to remove the unreacted agents, and the product was redispersed in DMF in the form of a paste. Finally, a small amount of the SWCNT paste was directly mixed with the aqueous AgNW suspension to obtain the stable AgNW/SWCNT mixture. The transparent conducting films were fabricated by depositing the prepared solutions onto polycarbonate substrates using an automatic spray coater (NCS Co. Ltd., NCS-400) with a 1.2 mm diameter nozzle and 400 \times 400 mm² stage.

Fabrication of the AgNW and AgNW/SWCNT hybrid film heaters. The transparent film heaters were fabricated in a two-terminal side-contact configuration. The DC voltage was supplied by a power supply to the film heater through a screen-printed silver contact at the film edge. The temperature of the film was measured using an IR thermal imager and a thermocouple located on the film. To fabricate the thermochromic display, we sprayed colored Chameleon® reversible thermochromic inks through shadow masks onto the thin film heater.

MW irradiation of the film. The films on the plastic substrates were placed inside a MW applicator, containing a moving metal short and a rectangular parallelepiped waveguide. A MW generator (PM740T, Richardson Electronics, Ltd.) supplied a power of 150–300 W at a frequency of 2450 MHz to the films. The surface temperatures of the films were measured using an infrared optical sensor (MI3-LT, Raytek).

Characterisation. The surfaces morphologies of the samples were imaged by field-emission scanning electron microscopy (Hitachi S4800). The structural characteristics of the AgNW and AgNW/SWCNT hybrid films were investigated by confocal Raman spectrometry (Ntegra Spectra, NT-MDT) with an excitation wavelength of 633 nm. The transmittance of each film was measured using a Varian Cary winUV spectrometer. The sheet resistance measurements were collected using a four-probe tester (Loresta, MCP-T610). The work functions of the AgNWs, UHP-SWCNTs, UHP-SWCNTs treated at 250 °C 1 h under vacuum were obtained from ultraviolet photoelectron spectroscopy (UPS; AXISNOVA, KratosInc.).

- Lee, J.-Y., Connor, S. T., Cui, Y. & Peumans, P. Solution-processed metal nanowire mesh transparent electrodes. *Nano Lett.* **8**, 689–692 (2008).
- De, S. *et al.* Silver nanowire networks as flexible transparent, conducting films: Extremely high DC to optical conductivity ratios. *ACS Nano* **3**, 1767–1774 (2009).
- Ellmer, K. Past achievements and future challenges in the development of optically transparent electrodes. *Nature Photon.* **6**, 809–817 (2012).
- Mutiso, R. M. *et al.* Integrating simulations and experiments to predict sheet resistance and optical transmittance in nanowire films for transparent conductors. *ACS Nano* **7**, 7654–7663 (2013).
- Hu, L., Hecht, D. S. & Grüner, G. Percolation in transparent and conducting carbon nanotube Networks. *Nano Lett.* **4**, 2513–2517 (2004).
- Dan, B., Irvin, G. C. & Pasquali, M. Continuous and scalable fabrication of transparent conducting carbon nanotube films. *ACS Nano* **3**, 835–843 (2009).
- Nirmalraj, P. N. *et al.* Electrical conductivity in single-walled carbon nanotube networks. *Nano Lett.* **9**, 3890–3895 (2009).
- Han, J. T. *et al.* Modulating conductivity, environmental stability of transparent conducting nanotube films on flexible substrates by interfacial engineering. *ACS Nano* **4**, 4551–4558 (2010).
- Garnett, E. C. *et al.* Self-limited plasmonic welding of silver nanowire junctions. *Nature Mater.* **11**, 241–249 (2012).
- Coskun, S., Ates, E. S. & Unalan, H. E. Optimization of silver nanowire networks for polymer light emitting diode electrodes. *Nanotechnology* **24**, 125202/1–8 (2013).

- Zhao, J., Sun, H., Dai, S., Wang, Y. & Zhu, J. Electrical breakdown of nanowires. *Nano Lett.* **11**, 1647–1651 (2011).
- Khaligh, H. H. & Goldthorpe, I. A. Failure of silver nanowire transparent electrodes under current flow. *Nanoscale Res. Lett.* **8**, 235/1–6 (2013).
- Peng, P. *et al.* Self-Oriented Nanojoining of Silver Nanowires via Surface Selective Activation. *Part. Part. Syst. Charact.* **30**, 420–426 (2013).
- Tokuno, T., Nogi, M., Jiu, J. & Suganuma, K. Hybrid transparent electrodes of silver nanowires and carbon nanotubes: a low-temperature solution process. *Nanoscale Res. Lett.* **7**, 281/1–7 (2012).
- Kim, D. *et al.* Transparent flexible heater based on hybrid of carbon nanotubes and silver nanowires. *Carbon* **63**, 530–536 (2013).
- Ahn, Y., Jeong, Y. & Lee, Y. Improved thermal oxidation stability of solution-processable silver nanowire transparent electrode by reduced graphene oxide. *ACS Appl. Mater. & Interf.* **4**, 6410–6414 (2012).
- Khomanov, I. N. *et al.* Reduced graphene oxide/copper nanowire hybrid films as high-performance transparent electrodes. *ACS Nano* **7**, 1811–1816 (2013).
- Tien, H.-W. *et al.* Using self-assembly to prepare a graphene-silver nanowire hybrid film that is transparent and electrically conductive. *Carbon* **58**, 198–207 (2013).
- Liu, Y., Chang, Q. & Huang, L. Transparent, flexible conducting graphene hybrid films with a subpercolating network of silver nanowires. *J. Mater. Chem. C* **1**, 2970–2974 (2013).
- Lee, M.-S. *et al.* High-performance, transparent, and stretchable electrodes using graphene-metal nanowire hybrid structures. *Nano Lett.* **13**, 2814–2821 (2013).
- Moon, I. K. *et al.* 2D graphene oxide nanosheets as an adhesive over-coating layer for flexible transparent conductive electrodes. *Sci. Rep.* **3**, 1112; DOI:10.1038/srep01112 (2013).
- Chen, R. *et al.* Co-percolating graphene-wrapped silver nanowire network for high performance, highly stable transparent conducting electrodes. *Adv. Func. Mater.* **23**, 5150–5158 (2013).
- Kim, T. Y. *et al.* Uniformly interconnected silver-nanowire networks for transparent film heaters. *Adv. Func. Mater.* **23**, 1250–1255 (2013).
- Zülicher, K. *et al.* Highly robust indium-free transparent conductive electrodes based on composites of silver nanowires and conductive metal oxide. *Adv. Func. Mater.* DOI: 10.1002/adfm.201303108 (2013).
- Zhu, R. *et al.* Fused silver nanowires with metal oxide nanoparticles and organic polymers for highly transparent conductors. *ACS Nano* **5**, 9877–9882 (2011).
- Kim, A. *et al.* Highly transparent low resistance ZnO/Ag nanowire/ZnO composite electrode for thin film solar cells. *ACS Nano* **7**, 1081–1091 (2013).
- Han, J. T. *et al.* Dispersant-free conducting pastes for flexible and printed nanocarbon electrodes. *Nature Commun.* **4**, 2491; DOI: 10.1038/ncomms3491 (2013).
- Lim, S. C. *et al.* Contact resistance between metal and carbon nanotube interconnects: Effect of work function and wettability. *Appl. Phys. Lett.* **95**, 264103/1–3 (2009).
- Han, J. T. *et al.* Self-passivation of transparent single-walled carbon nanotube films on plastic substrates by microwave-induced rapid nanowelding. *Appl. Phys. Lett.* **100**, 163120/1–4 (2013).

Acknowledgments

This research was supported by the Center for Advanced Soft Electronics under the Global Frontier Research Program of the Ministry of Science, ICT, and Future Planning as Global Frontier Project (CASE-2013M3A6A5073177), and by the Primary Research Program of Korea Electrotechnology Research Institute, South Korea.

Author contributions

J.S.W. and J.T.H. contributed equally to this work. J.S.W. carried out the experiment and wrote the manuscript. J.T.H. conceived and supervised the experiment and wrote the manuscript. S.J. performed the microwave irradiation test. J.I.J. and H.Y.K. performed the characterization of the film. H.J.J., S.Y.J., and K.-J.B. analyzed the data. G.-W.L. supervised the experiment and discussed the data. All authors discussed the results and commented on the manuscript.

Additional information

Supplementary information accompanies this paper at <http://www.nature.com/scientificreports>

Competing financial interests: The authors declare no competing financial interests.

How to cite this article: Woo, J.S. *et al.* Electrically Robust Metal Nanowire Network Formation by In-Situ Interconnection with Single-Walled Carbon Nanotubes. *Sci. Rep.* **4**, 4804; DOI:10.1038/srep04804 (2014).



This work is licensed under a Creative Commons Attribution-NonCommercial-NoDerivs 3.0 Unported License. The images in this article are included in the article's Creative Commons license, unless indicated otherwise in the image credit; if the image is not included under the Creative Commons license, users will need to obtain permission from the license holder in order to reproduce the image. To view a copy of this license, visit <http://creativecommons.org/licenses/by-nc-nd/3.0/>